

Search for New Physics in the Two Higgs to Four b-quark Final State

by

Alice Cocoros

**A dissertation submitted to The Johns Hopkins University
in conformity with the requirements for the degree of
Doctor of Philosophy**

Baltimore, Maryland

June, 2017

© Alice Cocoros 2017

All rights reserved

Abstract

My thesis is about bla bla

Primary Reader: Petar Maksimovic

Secondary Reader: Morris Swartz

Acknowledgments

Thanks!

Table of Contents

Abstract	ii
Acknowledgments	iii
Table of Contents	iv
List of Tables	v
List of Figures	vi
1 Introduction	1
1.1 The Standard Model	2
1.1.1 The Leptons	5
1.1.2 The Hadrons	6
1.1.3 The Forces	7
1.1.4 The Electromagnetic Force:	11
1.1.5 The Strong Force:	11
1.1.6 The Weak Force:	15
1.1.7 Mass and the Higgs Boson	18

1.2	Rounding Up the Standard Model Particles	20
1.2.1	The top quark	22
1.3	A Few Open Questions	23
2	Beyond The Standard Model	25
3	Particle Detection	26
3.1	The Large Hadron Collider	29
3.1.1	A proton-proton Collision	31
3.2	The Compact Muon Solenoid	34
3.3	Coordinates	37
3.3.1	The Subdetectors	38
3.3.1.1	The Tracker	38
3.3.1.2	The Calorimeters	39
3.3.1.3	The Solenoid	40
3.3.1.4	The Muon Chambers	41
3.3.2	The Particle Flow Algorithm	41
3.3.3	Jets	42
3.3.4	Triggers	45
3.3.5	Pileup	46

List of Tables

List of Figures

1.1	Snapshot of a cloud chamber, circa 1933: the vertical line represents a positron traveling through the cloud chamber, curving due to the magnetic field applied to the chamber.	1
1.2	The Lagrangian of the Standard Model.	3
1.3	The Standard Model. Image taken from CERN SMT able	4
1.4	$S^{\{2\}}$ represented as a Feynman Diagram. Each term in the equation corresponds to either a propagator (a line) or a vertex (a “corner”). The terms $\underline{A_\mu(x)A_\nu(x')}$ is the integral term. . . .	8
1.5	A Feynman Diagram depicting the interaction of two electrons. The action of the electromagnetic force is equivalent to the exchange of a photon. The vertical axis represents the distance between the electrons and the horizontal axis the passage of time.	9
1.6	A Feynman Diagram depicting the annihilation of a positron and an electron.	10
1.7	Simple electromagnetic vertex describing the interaction of two electrons and a photon.	10

1.8	Annihilation of an electron and a positron to create a muon and anti-muon. Backwards going arrows are often used in lieu of charges to denote anti-particles.	11
1.9	Three vertexes arising from QCD interactions. The curly line represents gluons. Note that gluons, which are colored, may interact with themselves.	12
1.10	Vertexes arising from weak interactions. The wavy lines represent the Bosons. The straight lines represent any particle where the appropriate quantities are conserved (details in the text). . .	16
1.11	Sketch of the Higgs Potential. Notice that while the over-all shape is symmetric about the y-axis, the function is not symmetric about the minima.	18
1.12	The Higgs Vertex. The dashed line is the Higgs Boson and the straight lines represent any massive particle (including the Higgs).	20
1.13	Collider Example: two quarks collide and form a gluon, which decays to two top quarks.	20
1.14	Some more Feynman Diagrams representing real physics processes. Some of these play real roles in modern analyses and some of these were constructed for the sake of the diagram itself.	22
1.15	Production of a Higgs boson from the collision of two gluons (which, notably, cannot couple directly to the Higgs). The triangular structure is a <i>loop</i>	23

3.1	Fluxes of common particles created in the atmosphere by cosmic rays. Note that muons are the most common charged particles produced in these interactions.	27
3.2	(left) Schematic of the LHC and the smaller accelerators which feed it. (right) True size of the LHC. The main ring has a circumference of 27 km. Lake Geneva can be seen in the top right of the picture.	30
3.3	Quadrupole magnetic field, with the direction of the force felt by a charged particle in the field shown in blue. Alternating the N and S faces of the magnets allows the fields to focus a particle beam in both the vertical and horizontal directions. . .	31
3.4	PDF for 10 GeV and 10 TeV collisions. Each curve represents a particle parton in a proton, and tells us the probability density of finding that parton carrying momentum fraction x	33
3.5	The Compact Muon Solenoid.	35
3.6	Schematic view of the CMS detector. Each portion is described in the text.	36
3.7	η and its relation to θ	37
3.8	The Hadronic Calorimeter, composed of 600 tons of brass, mostly recycled from WW2 naval shells.	40
3.9	Energy resolution gain from combining all information in the detector using the PF algorithm compared to that achievable with just the hadronic calorimeter.	41

3.10 Typical CMS event with large number of hadrons (shown by the green lines). These hadrons are collected into <i>jets</i> (shown by yellow triangles). The PF algorithm combines information from the trackers and calorimeters to properly measure the total momentum of the jet.	43
3.11 Four different <i>clustering</i> algorithms, each run on the same event. We use the <i>Anti-K_T</i> algorithm, described further in the text. . .	44
3.12 Resolution of $R = 1.0$ jets from different algorithms. The <i>Anti-K_T</i> Algorithm performs best.	48

Chapter 1

Introduction

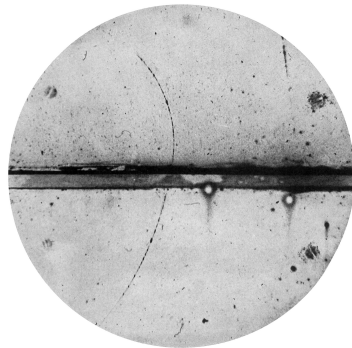


Figure 1.1: Snapshot of a cloud chamber, circa 1933: the vertical line represents a positron traveling through the cloud chamber, curving due to the magnetic field applied to the chamber.

In 1869, Johann Wilhelm Hittorf discovered Cathode Rays **cathode** suggesting that there may be subatomic particles. By 1911, these were identified as electrons, observed in many different ways, including cloud chambers, as can be seen in Figure 1.1. Soon after, protons were discovered in 1917, followed by neutrons in 1935.

As physicists advanced the study of quantum mechanics, many new particles were discovered. These particles can be broken down into several elementary particles, whose interactions are governed by *The Standard Model*

(SM).

1.1 The Standard Model

The SM describes the interaction of all elementary particles with one formula, shown in Figure 1.2. This lengthy Lagrangian can be summarized as a list of particles and mediating forces, represented in Figure 1.3.

$$\begin{aligned}
& -\frac{1}{2}\partial_\nu g_\mu^a \partial_\nu g_\mu^a - g_s f^{abc} \partial_\mu g_\nu^a g_\mu^b g_\nu^c - \frac{1}{4}g_s^2 f^{abc} f^{ade} g_\mu^b g_\nu^c g_\mu^d g_\nu^e + \\
& \frac{1}{2}ig_s^2 (\bar{q}_i^\sigma \gamma^\mu q_j^\sigma) g_\mu^a + \bar{G}^a \partial^2 G^a + g_s f^{abc} \partial_\mu G^a G^b g_\mu^c - \partial_\nu W_\mu^+ \partial_\nu W_\mu^- - \\
& M^2 W_\mu^+ W_\mu^- - \frac{1}{2} \partial_\nu Z_\mu^0 \partial_\nu Z_\mu^0 - \frac{1}{2c_w^2} M^2 Z_\mu^0 Z_\mu^0 - \frac{1}{2} \partial_\mu A_\nu \partial_\mu A_\nu - \frac{1}{2} \partial_\mu H \partial_\mu H - \\
& \frac{1}{2} m_h^2 H^2 - \partial_\mu \phi^+ \partial_\mu \phi^- - M^2 \phi^+ \phi^- - \frac{1}{2} \partial_\mu \phi^0 \partial_\mu \phi^0 - \frac{1}{2c_w^2} M \phi^0 \phi^0 - \beta_h [\frac{2M^2}{g^2} + \\
& \frac{2M}{g} H + \frac{1}{2}(H^2 + \phi^0 \phi^0 + 2\phi^+ \phi^-)] + \frac{2M^4}{g^2} \alpha_h - ig c_w [\partial_\nu Z_\mu^0 (W_\mu^+ W_\nu^- - \\
& W_\nu^+ W_\mu^-) - Z_\mu^0 (W_\mu^+ \partial_\nu W_\mu^- - W_\mu^- \partial_\nu W_\mu^+) + Z_\mu^0 (W_\nu^+ \partial_\nu W_\mu^- - \\
& W_\nu^- \partial_\nu W_\mu^+)] - ig s_w [\partial_\nu A_\mu (W_\mu^+ W_\nu^- - W_\nu^+ W_\mu^-) - A_\nu (W_\mu^+ \partial_\nu W_\mu^- - \\
& W_\mu^- \partial_\nu W_\mu^+) + A_\mu (W_\nu^+ \partial_\nu W_\mu^- - W_\nu^- \partial_\nu W_\mu^+)] - \frac{1}{2} g^2 W_\mu^+ W_\mu^- W_\nu^+ W_\nu^- + \\
& \frac{1}{2} g^2 W_\mu^+ W_\nu^- W_\mu^- W_\nu^+ + g^2 c_w^2 (Z_\mu^0 W_\mu^+ Z_\nu^0 W_\nu^- - Z_\mu^0 Z_\mu^0 W_\nu^+ W_\nu^-) + \\
& g^2 s_w^2 (A_\mu W_\mu^+ A_\nu W_\nu^- - A_\mu A_\nu W_\nu^+ W_\mu^-) + g^2 s_w c_w [A_\mu Z_\nu^0 (W_\mu^+ W_\nu^- - \\
& W_\nu^+ W_\mu^-) - 2A_\mu Z_\mu^0 W_\nu^+ W_\nu^-] - g\alpha [H^3 + H\phi^0 \phi^0 + 2H\phi^+ \phi^-] - \\
& \frac{1}{8} g^2 \alpha_h [H^4 + (\phi^0)^4 + 4(\phi^+ \phi^-)^2 + 4(\phi^0)^2 \phi^+ \phi^- + 4H^2 \phi^+ \phi^- + 2(\phi^0)^2 H^2] - \\
& g M W_\mu^+ W_\mu^- H - \frac{1}{2} g \frac{M}{c_w^2} Z_\mu^0 Z_\mu^0 H - \frac{1}{2} ig [W_\mu^+ (\phi^0 \partial_\mu \phi^- - \phi^- \partial_\mu \phi^0) - \\
& W_\mu^- (\phi^0 \partial_\mu \phi^+ - \phi^+ \partial_\mu \phi^0)] + \frac{1}{2} g [W_\mu^+ (H \partial_\mu \phi^- - \phi^- \partial_\mu H) - W_\mu^- (H \partial_\mu \phi^+ - \\
& \phi^+ \partial_\mu H)] + \frac{1}{2} g \frac{1}{c_w} (Z_\mu^0 (H \partial_\mu \phi^0 - \phi^0 \partial_\mu H) - ig \frac{s_w^2}{c_w} M Z_\mu^0 (W_\mu^+ \phi^- - W_\mu^- \phi^+) + \\
& ig s_w M A_\mu (W_\mu^+ \phi^- - W_\mu^- \phi^+) - ig \frac{1-2c_w^2}{2c_w} Z_\mu^0 (\phi^+ \partial_\mu \phi^- - \phi^- \partial_\mu \phi^+) + \\
& ig s_w A_\mu (\phi^+ \partial_\mu \phi^- - \phi^- \partial_\mu \phi^+) - \frac{1}{4} g^2 W_\mu^+ W_\mu^- [H^2 + (\phi^0)^2 + 2\phi^+ \phi^-] - \\
& \frac{1}{4} g^2 \frac{c_w^2}{c_w} Z_\mu^0 Z_\mu^0 [H^2 + (\phi^0)^2 + 2(2s_w^2 - 1)^2 \phi^+ \phi^-] - \frac{1}{2} g^2 \frac{s_w^2}{c_w} Z_\mu^0 \phi^0 (W_\mu^+ \phi^- + \\
& W_\mu^- \phi^+) - \frac{1}{2} ig \frac{s_w^2}{c_w} Z_\mu^0 H (W_\mu^+ \phi^- - W_\mu^- \phi^+) + \frac{1}{2} g^2 s_w A_\mu \phi^0 (W_\mu^+ \phi^- + \\
& W_\mu^- \phi^+) + \frac{1}{2} ig^2 s_w A_\mu H (W_\mu^+ \phi^- - W_\mu^- \phi^+) - g^2 \frac{s_w}{c_w} (2c_w^2 - 1) Z_\mu^0 A_\mu \phi^+ \phi^- - \\
& g^1 s_w^2 A_\mu A_\mu \phi^+ \phi^- - \bar{e}^\lambda (\gamma \partial + m_e^\lambda) e^\lambda - \bar{\nu}^\lambda \gamma \partial \nu^\lambda - \bar{u}_j^\lambda (\gamma \partial + m_u^\lambda) u_j^\lambda - \\
& d_j^\lambda (\gamma \partial + m_d^\lambda) d_j^\lambda + ig s_w A_\mu [-(\bar{e}^\lambda \gamma^\mu e^\lambda) + \frac{2}{3} (\bar{u}_j^\lambda \gamma^\mu u_j^\lambda) - \frac{1}{3} (\bar{d}_j^\lambda \gamma^\mu d_j^\lambda)] + \\
& \frac{ig}{4c_w} Z_\mu^0 [(\bar{\nu}^\lambda \gamma^\mu (1 + \gamma^5) \nu^\lambda) + (\bar{e}^\lambda \gamma^\mu (4s_w^2 - 1 - \gamma^5) e^\lambda) + (\bar{u}_j^\lambda \gamma^\mu (\frac{4}{3}s_w^2 - \\
& 1 - \gamma^5) u_j^\lambda) + (\bar{d}_j^\lambda \gamma^\mu (1 - \frac{8}{3}s_w^2 - \gamma^5) d_j^\lambda)] + \frac{ig}{2\sqrt{2}} W_\mu^+ [(\bar{\nu}^\lambda \gamma^\mu (1 + \gamma^5) e^\lambda) + \\
& (\bar{u}_j^\lambda \gamma^\mu (1 + \gamma^5) C_{\lambda\kappa} d_j^\kappa)] + \frac{ig}{2\sqrt{2}} W_\mu^- [(\bar{e}^\lambda \gamma^\mu (1 + \gamma^5) \nu^\lambda) + (\bar{d}_j^\kappa C_{\lambda\kappa}^\dagger \gamma^\mu (1 + \\
& \gamma^5) u_j^\lambda)] + \frac{ig}{2\sqrt{2}} \frac{m_e^\lambda}{M} [-\phi^+ (\bar{\nu}^\lambda (1 - \gamma^5) e^\lambda) + \phi^- (\bar{e}^\lambda (1 + \gamma^5) \nu^\lambda)] - \\
& \frac{g}{2} \frac{m_e^\lambda}{M} [H (\bar{e}^\lambda e^\lambda) + i\phi^0 (\bar{e}^\lambda \gamma^5 e^\lambda)] + \frac{ig}{2M\sqrt{2}} \phi^+ [-m_d^\kappa (\bar{u}_j^\lambda C_{\lambda\kappa} (1 - \gamma^5) d_j^\kappa)] + \\
& m_u^\lambda (\bar{u}_j^\lambda C_{\lambda\kappa} (1 + \gamma^5) d_j^\kappa) + \frac{ig}{2M\sqrt{2}} \phi^- [m_d^\lambda (\bar{d}_j^\lambda C_{\lambda\kappa}^\dagger (1 + \gamma^5) u_j^\kappa) - m_u^\kappa (\bar{d}_j^\lambda C_{\lambda\kappa}^\dagger (1 - \\
& \gamma^5) u_j^\kappa)] - \frac{g}{2} \frac{m_u^\lambda}{M} H (\bar{u}_j^\lambda u_j^\lambda) - \frac{g}{2} \frac{m_d^\lambda}{M} H (\bar{d}_j^\lambda d_j^\lambda) + \frac{ig}{2} \frac{m_u^\lambda}{M} \phi^0 (\bar{u}_j^\lambda \gamma^5 u_j^\lambda) - \\
& \frac{ig}{2} \frac{m_d^\lambda}{M} \phi^0 (\bar{d}_j^\lambda \gamma^5 d_j^\lambda) + \bar{X}^+ (\partial^2 - M^2) X^+ + \bar{X}^- (\partial^2 - M^2) X^- + \bar{X}^0 (\partial^2 - \\
& \frac{M^2}{c_w^2}) X^0 + \bar{Y} \partial^2 Y + ig c_w W_\mu^+ (\partial_\mu \bar{X}^0 X^- - \partial_\mu \bar{X}^+ X^0) + ig s_w W_\mu^+ (\partial_\mu \bar{Y} X^- - \\
& \partial_\mu \bar{X}^+ Y) + ig c_w W_\mu^- (\partial_\mu \bar{X}^- X^0 - \partial_\mu \bar{X}^0 X^+) + ig s_w W_\mu^- (\partial_\mu \bar{X}^- Y - \\
& \partial_\mu \bar{Y} X^+) + ig c_w Z_\mu^0 (\partial_\mu \bar{X}^+ X^+ - \partial_\mu \bar{X}^- X^-) + ig s_w A_\mu (\partial_\mu \bar{X}^+ X^+ - \\
& \partial_\mu \bar{X}^- X^-) - \frac{1}{2} g M [\bar{X}^+ X^+ H + \bar{X}^- X^- H + \frac{1}{c_w^2} \bar{X}^0 X^0 H] + \\
& \frac{1-2c_w^2}{2c_w} ig M [\bar{X}^+ X^0 \phi^+ - \bar{X}^- X^0 \phi^-] + \frac{1}{2c_w^2} ig M [\bar{X}^0 X^- \phi^+ - \bar{X}^0 X^+ \phi^-] + \\
& ig M s_w [\bar{X}^0 X^- \phi^+ - \bar{X}^0 X^+ \phi^-] + \frac{1}{2} ig M [X^+ X^+ \phi^0 - \bar{X}^- X^- \phi^0]
\end{aligned}$$

Figure 1.2: The Lagrangian of the Standard Model.

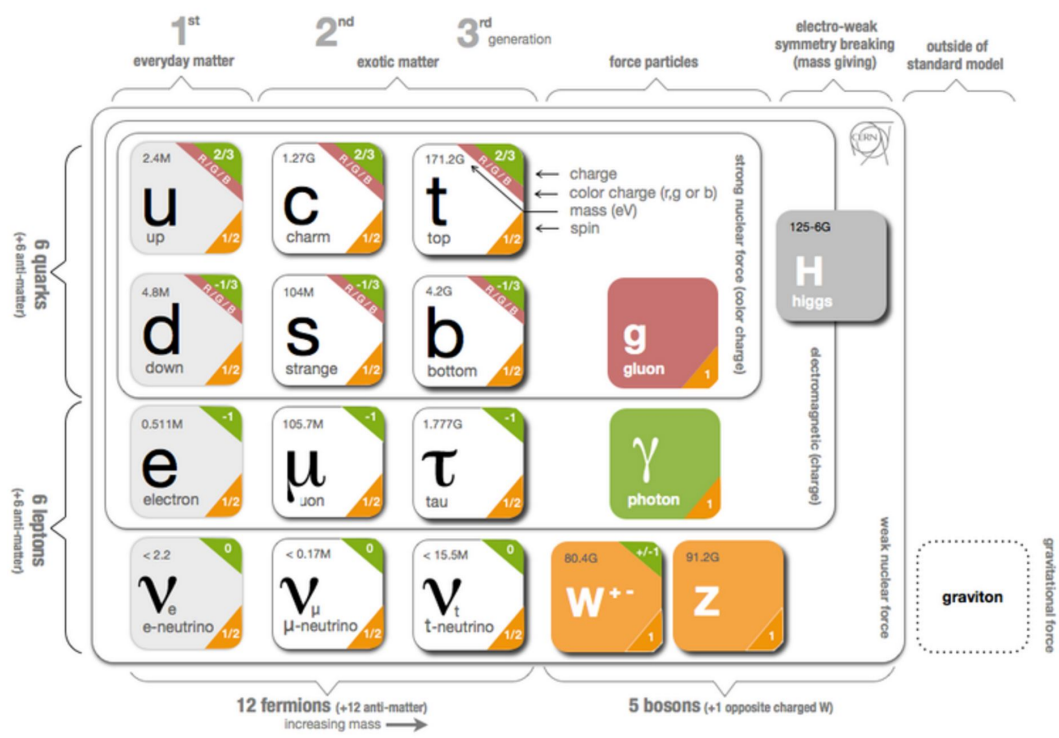


Figure 1.3: The Standard Model. Image taken from CERN SMTable

1.1.1 The Leptons

The electron is one of the most well known elementary particles. There exist two heavier “versions” of the electron: the muon (μ) which is ~ 200 times as massive as the electron, and the tau (τ) which is ~ 4000 times as massive as the electron. Each of these particles is negatively charged, where the charge is equivalent to -1 which corresponds to -1.602×10^{-19} Coulombs.

For each of these particles, there exists a corresponding neutrino, so we have ν_e , ν_μ and ν_τ . The neutrinos as defined by the SM are chargeless and massless, although experiments have proved that at least two out of three neutrinos observed in nature have mass.

A corresponding anti-particle exists for each of these six particles: \bar{e} (e^+), $\bar{\mu}$ (μ^+), $\bar{\tau}$ (τ^+), $\bar{\nu}_e$, $\bar{\nu}_\mu$, and $\bar{\nu}_\tau$. Note that, while neutrinos are chargeless, the anti-particle for the electron, muon, and tau, all have positive (or opposite of their corresponding particle) charge.

There is another property we must mention: the *spin*. Spin is the intrinsic angular momentum of the particle. The electron is a point particle, and there is therefore nothing actually revolving. Just as in the macro-world, there are two directions something can spin around an axis, which we denote as positive or negative spins. The spin is a vector quantity. The leptons all have spin $\frac{1}{2}$ (or $-\frac{1}{2}$), which means they are *fermions*.

The spin of a particle allows us to define one more property: the *helicity* (also called *handedness*). The helicity is defined as *the sign of the projection of the particle’s spin vector onto its momentum vector*. We usually refer to negative

helicity as left-handedness and positive helicity as right-handedness. Hand-edness might seem like a trivial quantity but it plays an important part in the actual calculations that are part of the Standard Model: left and right handed particles can behave differently. Indeed, while the massive leptons can be either left or right handed, it appears that all neutrinos are left-handed, and all anti-neutrinos are right handed. There is currently no explanation for this strange fact.

1.1.2 The Hadrons

The Standard Model constructs the myriad particles found in the last century (excluding of course the leptons) out of just six particles, called the quarks. Like the leptons they exist in three separate groups (called “generations”). They are: the *up* (*u*) and *down* (*d*) quarks, the *strange* (*s*) and *charm* (*c*) quarks, and the *bottom* (*b*) and *top* (*t*) quarks.

The *u*, *c* and *t* quarks have charge $+\frac{2}{3}$ and the *d*, *s* and *b* quarks have charge $-\frac{1}{3}$. Each has its own mass, and like the leptons they have antiparticles ($\bar{u}, \bar{d}, \bar{s}, \bar{c}, \bar{b}$ and \bar{t}), and spin. Like the leptons they have spin $\frac{1}{2}$ (or $-\frac{1}{2}$) and are therefore also fermions.

Unlike the leptons however, the quarks are colored¹. While there are two “kinds” of electric charge: positive and negative, color is a bit more complicated: quarks can be *red*, *green* or *blue*. Anti-quarks meanwhile can be *anti-red*, *anti-green* or *anti-blue*.

The electric charge can be detected directly, color cannot. Because of the

¹this is just a different kind of charge, it has nothing to do with the colors we experience visually

particularities of the force governing colored particles, the quarks always come bound together in color neutral combinations, either by combining all three colors (which count as neutral) or by combining a color and its anticolor. For example, the proton is the combination of two d and one u quarks. Each of these carries one of the distinct colors and the combination is neutral. The pion (π^+) is a combination of a u and a \bar{d} where the up quark would carry some color and the (anti-)down would carry that same anti-color. All the particles discovered in the 1900s were just combinations of the six quarks. The fractional charges of the quarks can never be directly detected as there are no colour neutral combinations which do not result in unit charge.

1.1.3 The Forces

Without some forces to hold all these pieces together, the universe would be a soup of quarks and leptons. In the Standard Model, forces are not “Actions at a Distance”, but rather, the exchange of *force mediating* particles.

Consider the most basic of particle interactions: two electrons are shot towards each other. Since they are both negatively charged, they repel each other. If we consider that the system starts in some state i and ends in some state f , the probability of the transition $i \rightarrow j$ happening is related to the infinite sum:

$$S_{fi} = \sum_{n=0}^{\infty} S^n \quad (1.1)$$

The sum is over orders of perturbation², where the first order $n = 1$ state is the case where the electrons do not interact at all. The next (and first interesting)

²Quantum Mechanics uses perturbation theory to move from a simple approximate solution to a more precise one.

term of S is:

$$S^{\{2\}} = \pm^{\{n\}} \bar{\psi}(x) i e \gamma^\mu \psi(x) \bar{\psi}(x') i e \gamma^\nu \psi(x') \int \frac{d^4 k}{(2\pi)^4} \frac{-g^{\mu\nu}}{k^2 - i0} e^{-ik(x-x')} \quad (1.2)$$

where the integral is over all the possible momenta of the incoming and outgoing electrons. This is just the first non-trivial term of the sum. Fortunately it is the dominant term. Unfortunately, a clear description of the process is hidden by the opaqueness of the mathematics. Enter the *Feynman diagram*. Each term in the expression for $S^{\{2\}}$ can be encoded in as a pictoral element of a Feynman Diagram (as shown in Figure 1.4). With the Feynman Diagram,

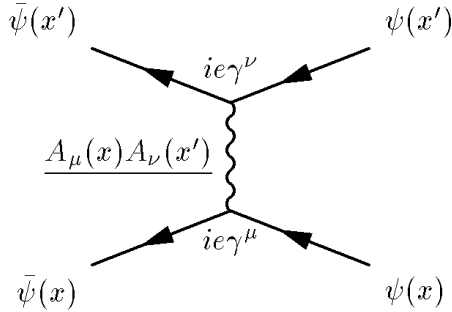


Figure 1.4: $S^{\{2\}}$ represented as a Feynman Diagram. Each term in the equation corresponds to either a propagator (a line) or a vertex (a “corner”). The terms $A_\mu(x)A_\nu(x')$ is the integral term.

we can explicitly refer to physical processes with an (exact) visual description. There is no loss of generality or rigor!

Returning to the specifics of our example; two electrons interacting: the entire (first order) interaction is encoded in the Feynman Diagram in Figure 1.5. The effect of the electromagnetic force is just the exchange of a photon³. The

³This model is of course, only valid on the very small scales (both in time and space) of particle physics. If we were to really shoot two electrons together in a laboratory, they would exchange a great many photons, not just one.

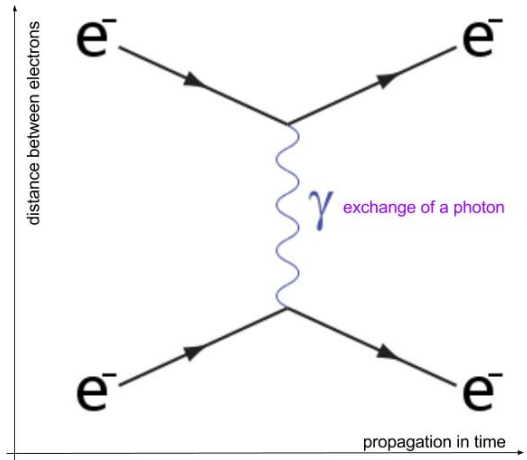


Figure 1.5: A Feynman Diagram depicting the interaction of two electrons. The action of the electromagnetic force is equivalent to the exchange of a photon. The vertical axis represents the distance between the electrons and the horizontal axis the passage of time.

Standard Model however doesn't just describe how particles interact. Indeed, the interaction we've just described could be described without any particle physics or even quantum mechanics. What the Standard Model allows us to do that previous formulations did not was account for the fact that particles can be created or destroyed. Consider for example the diagram in Figure 1.6. Here, an electron (e^-) and an anti-electron (e^+) are shot at each other. They annihilate, which is to say: they become (or merge into) a photon. Some time later, the photon decays into a new set of positrons and electrons. During this interaction charge was conserved, since the photon is chargeless and the electron/positron pair combined has $1 + -1 = 0$ charge.

These two processes are essentially equivalent. They are just different arrangements of the same *vertex*. A vertex is a point interaction between particles. In the case of electron-positron annihilation or electron-electron repulsion, the vertex is the same, and is shown in Figure 1.7. With just

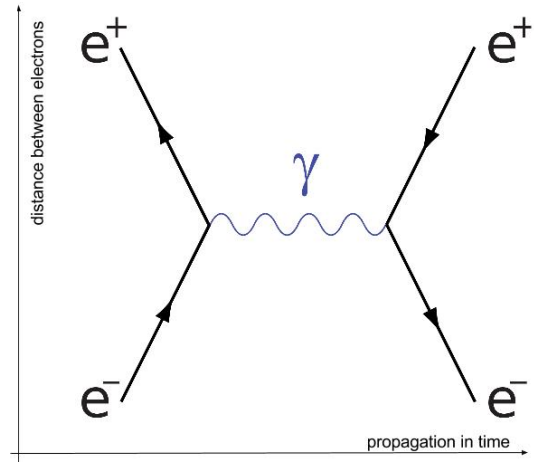


Figure 1.6: A Feynman Diagram depicting the annihilation of a positron and an electron.

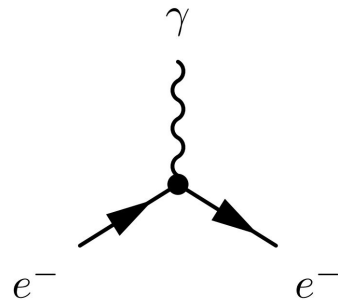


Figure 1.7: Simple electromagnetic vertex describing the interaction of two electrons and a photon.

this vertex, we can construct a huge number of possible electromagnetic interactions. In the diagrams, electrons and positrons are the same: a positron moving backward in time (in the negative time direction on the axis, so to the left in our diagrams) is the same as an electron moving forward in time. In the case of the photon, similar vertexes exist for any charged particle and it's (opposite sign) anti-particle. For example, muons can be produced via the process $e^+e^- \rightarrow \gamma \rightarrow \mu^+\mu^-$, whose Feynman diagram is shown in Figure 1.8. Now that we are armed with the Feynman Diagram, each force can be thought

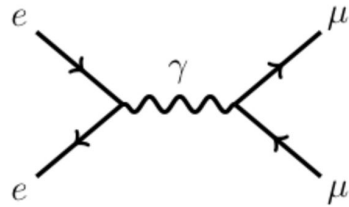


Figure 1.8: Annihilation of an electron and a positron to create a muon and anti-muon. Backwards going arrows are often used in lieu of charges to denote anti-particles.

of as some mediator particles with some rules governing which vertexes may be constructed. We will allow the Feynman Diagrams to obfuscate the computations, and focus on a qualitative description of these processes.

1.1.4 The Electromagnetic Force:

The field theory description of the Electromagnetic Force is called *quantum electrodynamics*, often abbreviated as *QED*. It describes how charges interact. QED with its carrier particle, the photon (γ), is the simplest of the fundamental forces described by the Standard Model. In fact, we've already described it fully, as the only vertex included is that in Figure 1.7. The photon is massless, and moves at the speed of light.

QED has been rigorously tested by a variety of experiments, with very little deviation from the behavior expected from the Standard Model⁴.

1.1.5 The Strong Force:

Quantum Chromodynamics (abbreviated to *QCD*) is the field theory of colored interactions. The force carrier is the *gluon* (g). The photon is chargeless, so it

⁴very little deviation here means truly minuscule deviations: differences on the order of 10/1,000,000,000ths of the predicted values, and well within the expected uncertainties of such measurements.

cannot couple to itself. The gluon however carries color; which means that there is more than one vertex in QCD. These vertexes are shown in Figure 1.9.

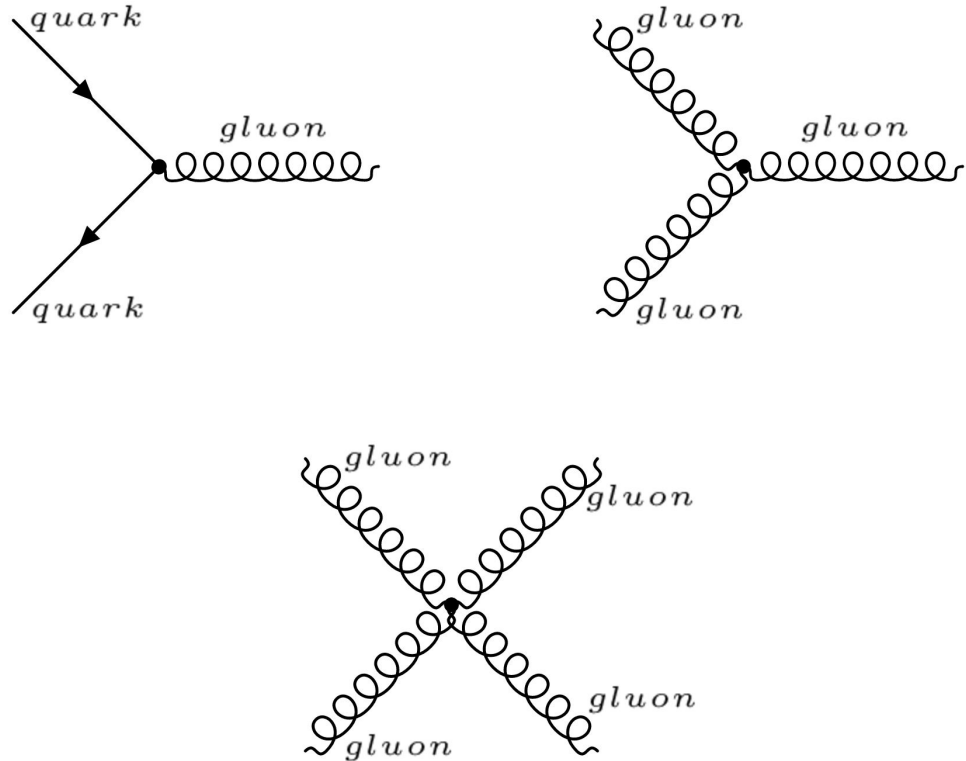


Figure 1.9: Three vertexes arising from QCD interactions. The curly line represents gluons. Note that gluons, which are colored, may interact with themselves.

Each quark carries one color (and each anti-quark carries one anti-color). Color is conserved, so for the diagrams in Figure 1.9 to work, the gluons must carry both a color and an anti-color. There is no $r\bar{r}$ (red + anti-red) gluon. Instead, we must delve a little bit into the behavior of the strong force.

While the protons and the neutrons (called nucleons) are confined to nuclei by the strong force, they are not colored the way the quarks are. This might seem like a contradiction, but it is not: the gluon is not the carrier

particle which binds the nucleons together. Instead, the nucleons exchange mesons (two-quark bound states) in the same way that two electrons might exchange photons. This is sometimes called the *residual strong force*, it's an emergent property of complex systems of colored particles. While the gluon is massless (and therefore, like the photon, not limited in range) the mesons are not, limiting the range over which this interaction can take place, and explaining why the strong force can't be felt the same way as the electric force.

The leptons are truly “colorless”, but while the protons and the neutrons behave similarly, they are a *color singlet*. The color singlet is the superposition⁵ of the quantum states:

$$\frac{r\bar{r} + b\bar{b} + g\bar{g}}{\sqrt{3}} \quad (1.3)$$

Singlets may interact with each other (this is what's happening when a pion travels between two nucleons). Since singlets may interact with each other, and there is no mass to limit the range of the gluon, we can be sure (empirically) that no gluons carry the singlet color state.

Gluons can take any of the remaining color combinations. Instead of writing them all down, we represent them with a linearly independent set from which all of them can be constructed:

$$\begin{array}{cccc} \frac{r\bar{b}+b\bar{r}}{\sqrt{2}} & \frac{r\bar{g}+g\bar{r}}{\sqrt{2}} & \frac{b\bar{g}+g\bar{b}}{\sqrt{2}} & \frac{r\bar{r}-b\bar{b}}{\sqrt{2}} \\ \frac{-i(r\bar{b}-b\bar{r})}{\sqrt{2}} & \frac{-i(r\bar{g}-g\bar{r})}{\sqrt{2}} & \frac{-i(b\bar{g}-g\bar{b})}{\sqrt{2}} & \frac{r\bar{r}+b\bar{b}-2g\bar{g}}{\sqrt{6}} \end{array}$$

These are the color *octet*. It is not the only such set possible, but there are

⁵In quantum mechanics, the results of measurements can be a superposition of states: for example, the color state $(r\bar{b} + b\bar{r})/\sqrt{2}$ corresponds to a gluon which is equally likely to be in the state red + anti-blue or blue + anti-red. The square root of two is a normalizing term to make the quantum mechanical calculations return probabilities less than one.

no combinations which are less complex. The octet must be constructed in such a way that it is impossible to get the singlet state.

What does happen if we try to forcibly separate a singlet state? For example, let's say that we smash an electron into a proton with sufficient force to temporarily overcome the strong force and one of its quarks is ejected?

The shards of the proton coming out of this collision all carry color, and are therefore able to interact with each other. If they only felt electric charges, they would simply exchange photons. Not so with the strong force: as the quarks drift away from each other, the carrier gluons, which can interact with each other) form a web between them. We call this object a *color tube*. The tube containing a jumble of self-interacting gluons. These tubes exert approximately constant force when stretched, increasing the energy in the tube until⁶ it becomes more energetically favorable to create a new pair of quarks out of the vacuum (through the top left vertex shown in Figure 1.9).

The result is that the quark that was drifting away, abhorrently not contained in a singlet state, suddenly finds itself paired with a new quark. If there isn't too much energy, these now stay bound and have become a meson. If the quark is still too energetic to be contained, then the process will repeat itself, chipping away at the energy of the original quark until every colored particle is collected in a singlet state. This property is called *containment*, and the process by which new quarks are produced to enforce it is called *hadronization*.

Hadronization plays a very important part in the experiment this Thesis will describe. It's relationship with particle detection is described in detail in

⁶at distances of about 10^{-15} , incidentally the roughly the radius of an atomic nucleus

Chapter 3.

1.1.6 The Weak Force:

In this very distant past, the Weak force and the Electromagnetic force were one. They were called the Electroweak Interaction, and there were four carrier particles, W_1 , W_2 , W_3 and B . All four of these were massless, and had unit spins (as such, they were *bosons*). While temperatures were high enough, these bosons were able to ignore the effects of the Higgs field, which we discuss in the next section.

As the universe cools down, the four bosons begin to interact with this field. The fermions now no longer interact directly with the W_1 , W_2 , W_3 and B , but rather, with superpositions of them. Where previously there were a B and a W_3 Boson, we now have, γ and Z . This superposition is simple to write:

$$\begin{pmatrix} \gamma \\ Z \end{pmatrix} = \begin{pmatrix} \cos \theta_W & \sin \theta_W \\ -\sin \theta_W & \cos \theta_W \end{pmatrix} \begin{pmatrix} B \\ W_3 \end{pmatrix} \quad (1.4)$$

Where θ_W called the Mixing Angle or Weinberg Angle, is a parameter of the Standard Model. The photons of the Electromagnetic force are just a particular combination of the B and W_3 . The Z Boson is one of the carrier particles of the Weak Force. Similarly ,the W_1 and W_2 bosons combine via the superposition

$$W^\pm = \frac{(W_1 \mp iW_2)}{\sqrt{2}} \quad (1.5)$$

to form two new Bosons, the W^+ and W^- .

We've already talked about the behavior of the photon, so we just need to detail the vertexes involving the W and Z bosons for a full description of

the Weak Force. These vertexes are shown in Figure 1.10. The Z Boson is

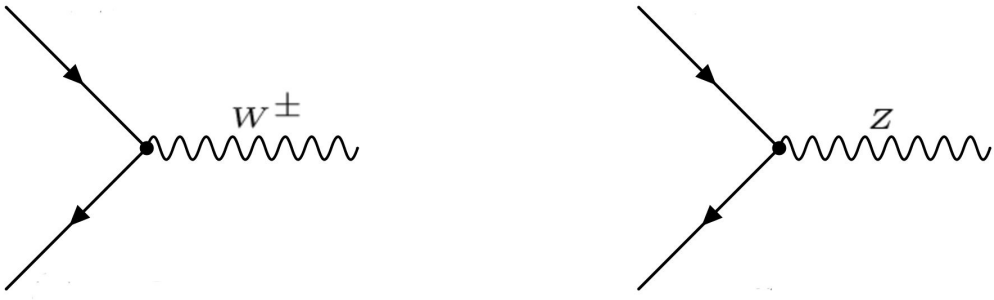


Figure 1.10: Vertexes arising from weak interactions. The wavy lines represent the Bosons. The straight lines represent any particle where the appropriate quantities are conserved (details in the text).

not massless, it has mass $91.2 \text{ GeV}/c^2$ ⁷. Z bosons couples particles to their anti-particles. For example, the process $Z \rightarrow e^-e^+$ is allowed but the process $Z \rightarrow \mu^+e^-$ is not. Similarly, $Z \rightarrow b\bar{b}$ is allowed but $Z \rightarrow b\bar{u}$ is not. In this regard, it behaves like a heavy version of the photon, except that it can couple to neutral particles (for example, $Z \rightarrow \nu_e\bar{\nu}_e$).

The W boson (with a mass of $80.4 \text{ GeV}/c^2$) also couples pairs of fermions, except that it links the flavors within a generation. For example, a W boson might decay to two quarks ($W \rightarrow u\bar{d}$) or to a lepton and its neutrino ($W \rightarrow \mu\nu_\mu$). It is charged, so the process $\gamma \rightarrow W^+W^-$ is allowed. The decay $Z \rightarrow W^+W^-$ is also allowed.

The W boson is a fascinating object to study. As we've already mentioned

⁷The unit GeV/c^2 is a unit of mass. One eV/c^2 is equal to $1.78 \times 10^{-36} \text{ kg}$. An electron has mass $\sim 0.5 \text{ MeV}/c^2$ and a proton $\sim 1 \text{ GeV}/c^2$.

in passing: The weak interaction only acts on left-handed particles and right-handed anti-particles⁸.

The decay $\gamma \rightarrow \mu^+ e^-$ is a perfectly plausible decay, seeing as charge is conserved. However, it never occurs. Similarly, the Z boson might be allowed to decay to different generation quarks (this wouldn't violate charge or color), but it simply does not happen. These decays are called *flavor changing neutral currents*. Flavor changing charged currents on the other hand, do exist. Specifically, Ws can decay to quark pairs outside of their generation. For example, we might see $W \rightarrow s\bar{u}$. The probability of a W decaying to different generations is encoded in the CKM Matrix, an empirically measured set of values. Here is that matrix:

$$\begin{pmatrix} V_{ud} & V_{us} & V_{ub} \\ V_{cd} & V_{cs} & V_{cb} \\ V_{td} & V_{ts} & V_{tb} \end{pmatrix} = \begin{pmatrix} 0.974 & 0.225 & 0.004 \\ 0.225 & 0.973 & 0.041 \\ 0.009 & 0.040 & 0.999 \end{pmatrix} \quad (1.6)$$

where $|V_{ij}|^2$ is the probability that a quark i decays to a quark j through the emission of a W.

It is then because of the W and the W only that our world seems to be composed of only up and down quarks and electrons. All other particles will eventually decay (through a W) to something lighter. The other leptons (the muons and the taus) will eventually decay by emitting a neutrino and a W, with the W decaying to an electron and a neutrino. All the various particles discovered in the last century eventually decayed to protons and neutrons because the higher order quarks embedded in them decayed (again, through

⁸This causes considerable complications because neutrinos have mass. It is therefore possible to define a reference frame in which the neutrino is moving backwards with relation to the W it decayed from, thus flipping its helicity...

a W) back to the first generation.

1.1.7 Mass and the Higgs Boson

The Higgs Boson is the most recent addition to the Standard Model to be discovered. It is responsible for giving the other particles their mass⁹. As we already mentioned, this does not happen at very high energies. To understand this, we should consider the Higgs Potential. For the purpose of illustration we can simplify it to the form $\sim (\phi^2 - \eta^2)^2$, where ϕ is the Higgs Field, which we plot in Figure 1.11¹⁰. The potential in question is symmetric (about the

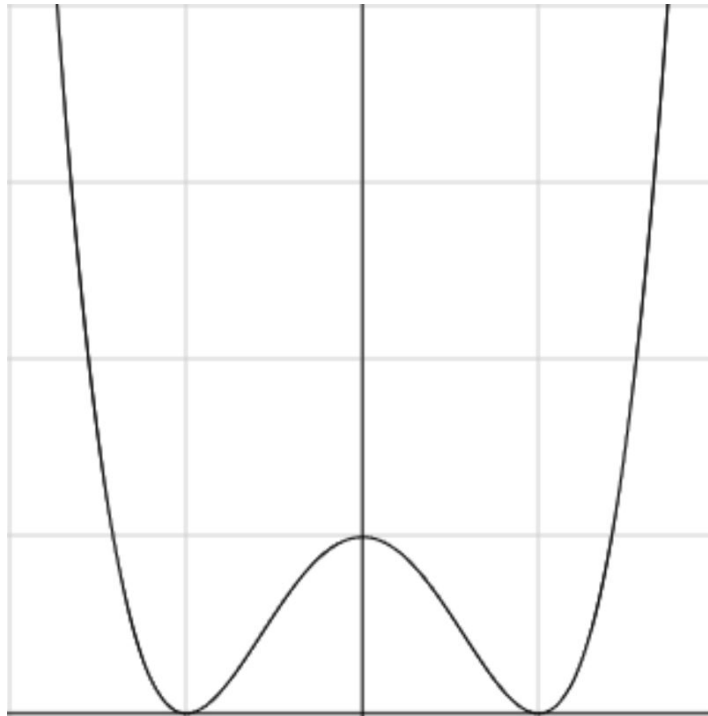


Figure 1.11: Sketch of the Higgs Potential. Notice that while the over-all shape is symmetric about the y-axis, the function is not symmetric about the minima.

⁹except the neutrinos, which by now you must have noticed, are devious...

¹⁰This shape is sometimes called the “mexican hat” or “champagne bottle” potential, depending on the level of cultural sensitivity required.

y-axis, which in the case of the actual Higgs potential would have units of energy). In the high-temperature early universe, the energies of particles was such that the "bump" at the bottom of the potential played no part. As the universe cools, however, things must settle into either of the two valleys. It's not the case that the equations of the Standard Model aren't symmetric, it's that practically, at the energies in question, they cause behavior which is not. This is called *spontaneous symmetry breaking*.

This asymmetry causes the Higgs field in the low temperature universe to take on a vacuum expectation value (roughly speaking: its average value in empty space) which is non-zero (it's 246 GeV). We usually abbreviate this as just the *VEV*. The VEV couples to the electroweak interactions, creating the photon and the weak force bosons as we experience them.

Through a similar but not identical process, this spontaneously broken Higgs field also couples to the weak bosons, quarks, electron, muon and tau, giving them mass where without it they were massless. The neutrinos do not couple, and are therefore massless in the standard model.

So far we've been talking about the Higgs field, but as you may have heard, there is also a Higgs Boson. This particle is just an excitation of the Higgs Field the way we think of a photon as being an excitation of the electromagnetic field. It was discovered in 2012 at the Large Hadron Collider after a 40 year long search. This Higgs has no charge, has no spin, and has a mass of 126 GeV. It couples to anything with mass, which means it couples to itself. The Higgs Vertex is the very last piece of the Standard Model, and is shown in Figure 1.12.

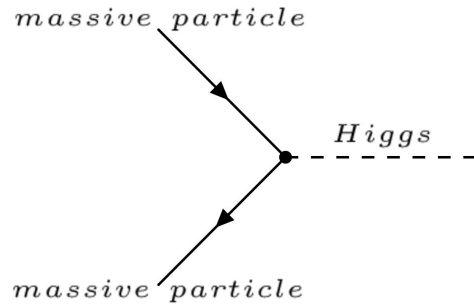


Figure 1.12: The Higgs Vertex. The dashed line is the Higgs Boson and the straight lines represent any massive particle (including the Higgs).

1.2 Rounding Up the Standard Model Particles

So to recap, there are, once we count all the colors and anti-particles, 61 particles in the standard model. We know they interact, and we can pictorially express a number of complex interactions using the Feynman diagram. For example, consider the diagram in Figure 1.13. This is an important physics

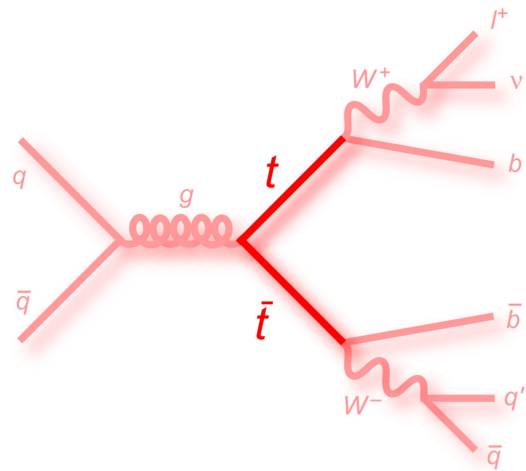


Figure 1.13: Collider Example: two quarks collide and form a gluon, which decays to two top quarks.

process¹¹ found in high energy colliders, and we'll discuss it in much more detail later on. For now, it serves as a useful example of the kind of processes we can construct with our Feynman diagrams: two protons collide and quarks inside of them annihilate¹² into a gluon. That gluon propagates some distance before it decays back to quarks, this time to a pair of top quarks. Each of these decays through Weak interactions to a b and a W (this is almost always the case, see Equation 1.6). One W decays to a lepton and a neutrino, and the other to a pair of quarks. This diagram then contains five distinct vertexes.

Indeed, we can make these diagrams as complicated as we want. Some of them become quite silly. See Figure 1.14 for some more entertaining examples.

We've given a mostly qualitative description of the model, without differentiating between facts gleaned from experiments and facts that come from calculations within the model itself. Fortunately, the Standard Model is extremely self-consistent and despite there being 61 particles, 4 forces and 1 Higgs field, there are only 19 "free parameters" which have to be determined experimentally. Most of them are masses. The Higgs Boson is the reason that the particles have mass, but it doesn't specify what those masses should be. What was the question "why does a particle have this mass" now becomes "why is this particle's coupling to the Higgs what it is". The CKM Matrix's nine entries can be interrelated with just four parameters. The remaining parameters have to do with the Higgs field or the couplings of the forces.

¹¹incidentally, the primary background of this Thesis' analysis

¹²See Chapter 3 for a more formal description of what's happening there

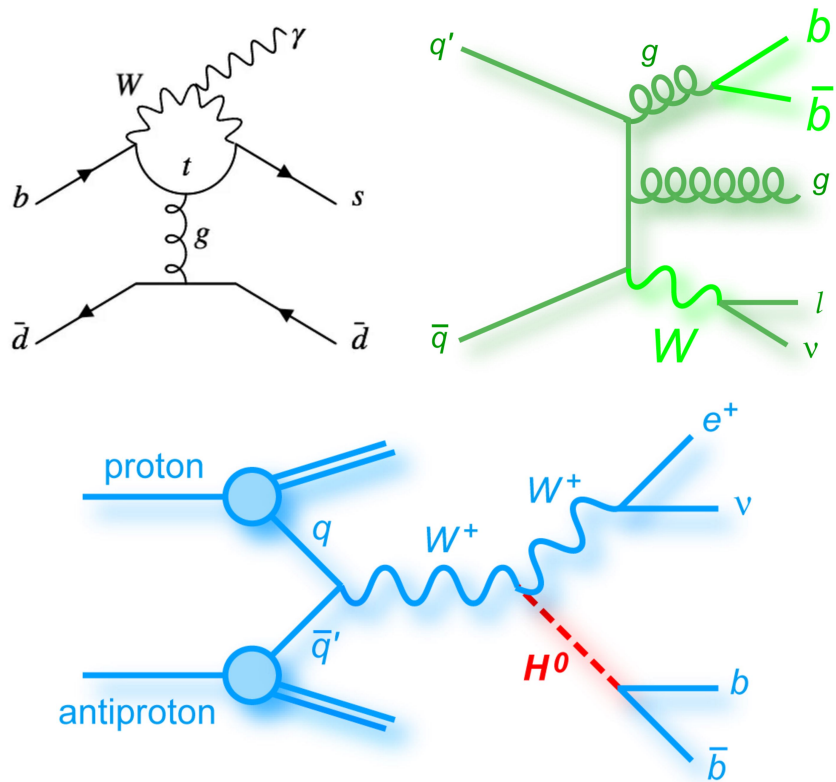


Figure 1.14: Some more Feynman Diagrams representing real physics processes. Some of these play real roles in modern analyses and some of these were constructed for the sake of the diagram itself.

1.2.1 The top quark

No discussion of the standard model is complete unless it mentions how strange the top quark is¹³. The top quark's mass is $174 \text{ GeV}/c^2$. The next heaviest quark barely makes it to the $5 \text{ GeV}/c^2$ mark, with all other fermions being lighter than it.

This might just be a curiosity, as there is nothing inherently “wrong” with a very heavy top, but it does lead to some strange behavior. The top quark

¹³even though it has strangeness 0.

is the only quark that can exist outside of a color singlet. This is because the color tubes we mentioned before never form: due to its very large mass, the top decays immediately (in 5×10^{-25} seconds) through the Weak force to a bottom quark (or very rarely, a c or a d) and a W Boson.

This does not mean that the top quark can only interact weakly, just that it decays that way. The top quark plays an important role in Higgs production (since the Higgs couples so strongly to it), as shown in Figure 1.15. As we will see, the top quark is a frequent player in searches for new physics as new theories often couple preferentially to massive objects.

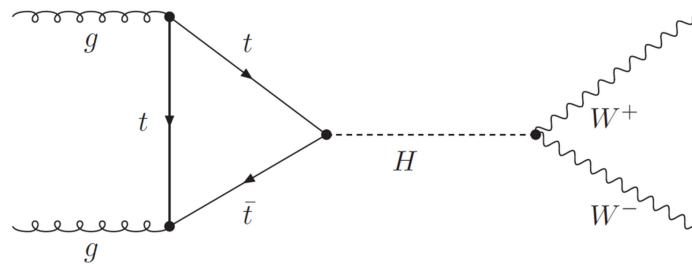


Figure 1.15: Production of a Higgs boson from the collision of two gluons (which, notably, cannot couple directly to the Higgs). The triangular structure is a *loop*.

1.3 A Few Open Questions

For a supposed Theory of Everything, the Standard Model could use some improvement. It only covers a slim 4.6% of the content of the known universe. Dark Matter, something completely outside the Standard Model, accounts for a further 24%, with the rest being mysterious Dark Energy. Both these Dark Entities loom as considerable proof that while the Standard Model does a good job of describing that little 4.6% we call *Baryonic Matter*, it is far from a

complete description of the world.

Actually, the Standard Model isn't even a complete description of Baryonic Matter. The obvious problem being of course, that it fails to explain, or in any way even include, the most obvious of forces: Gravity. Gravity is not included in the Standard Model. It's easy to just say that gravity just doesn't matter at the very small distances the Standard Model applies to, but the addition of some massless force-carrying *Graviton* would certainly be welcome.

Of course, there's also these pesky neutrinos and their unwarranted masses to directly (experimentally) challenge our model. These are not the only hints that we're missing something. One obvious observation is that while the Standard Model treats positrons and electrons (and quarks and anti-quarks) symmetrically, the universe's Baryonic Matter is overwhelmingly composed of electrons and quarks. What happened to all the anti-particles?

And what are these insanely energetic cosmic rays we detect from time to time? The Standard Model puts limits on the energy a cosmic ray can attain before it is slowed down by interactions in space... and yet, we have detected particles some orders of magnitude above that limits.

One of the great strengths of the Standard Model is that it is incredibly self-consistent. Indeed, it has been tested and re-tested, with no obvious internal flaw. Now however, as we start to seek the answer to new questions, this strength becomes a flaw as there is no way to modify the model without un-hinging some other internal aspect. To answer the questions of modern physics then, we must venture into new territory Beyond The Standard Model!

Chapter 2

Beyond The Standard Model

Chapter 3

Particle Detection

While particle physics has come a long way in the last century, the basic discovery mechanism hasn't changed: to get a new particle, smash known particles together. In the early days, this was achieved by simply waiting for cosmic rays¹ to enter our detectors.

For example, a positron might be accelerated by the Sun's tumultuous electromagnetic fields to very high energy and it might collide with an atom in our atmosphere. The positron might annihilate with one of the electrons in that atom (through the process in Figure 1.7). Even if the electron was at rest, the positron carried sufficient energy that the resulting photon could decay into something heavier than the electron: a pair of muons for example. This is exactly how muons are produced in the atmosphere, and in fact, at sea level every square meter is showered with about a hundred muons per second.

Other particles should be accessible this way, but as can be seen in Figure 3.1, their rates are considerably lower than the muon. We would need to wait a very long time to have enough Ws pass through our detector to have any

¹Charged particles ejected from the sun which strike our atmosphere

hope of making a reasonable measurement. The muon is relatively long-lived,

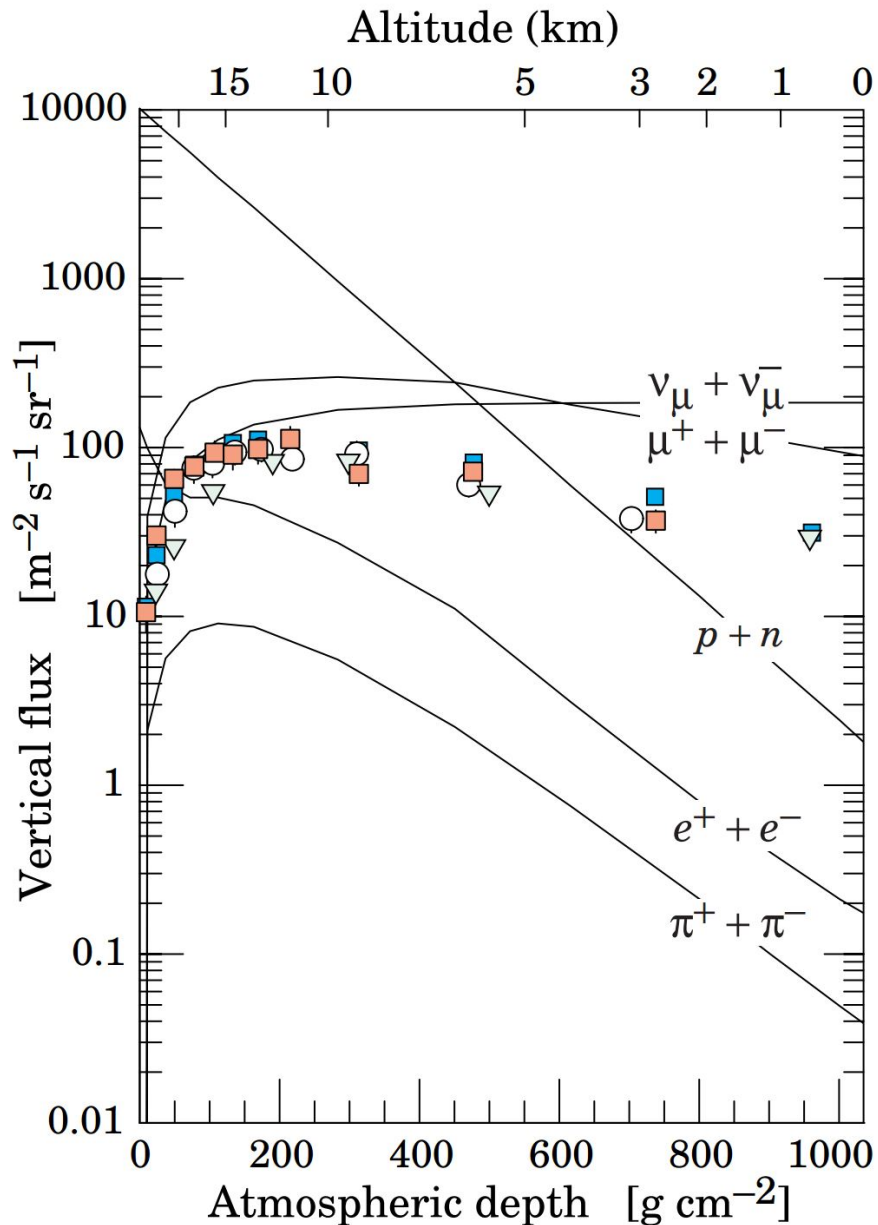


Figure 3.1: Fluxes of common particles created in the atmosphere by cosmic rays. Note that muons are the most common charged particles produced in these interactions.

while the bosons and heavier quarks would decay in flight. The muon only

makes it to our detectors because it is moving near the speed of light and benefits from the effects of time dilation².

Clearly then we need to force positron and electrons to collide on our terms, preferably at very high energies.

The most basic collider is a long, straight tunnel which fires a beam of electrons at a beam of positrons. Most of the positron and electrons will pass by each other, with only a few actually interacting. Because of this, it makes more sense to build circular rings spinning the particles in opposite directions. This way a bunch³ of electrons isn't wasted if it doesn't produce any interesting interactions with the positrons: it'll whip around the ring for a second pass, and a third, until it's depleted.

The *Large Electron-Positron Collider* at CERN was precisely such a machine, and was able to produce collisions with a center of mass energy of 206 GeV. More than enough energy to produce Z and W bosons (then the heaviest particles around). There are however some drawbacks to electron-positron colliders: charged particles radiate energy when they are bent by an electromagnetic field, according to the following formula:

$$P = \frac{e^4}{6\pi m^4 c^5} E^2 B^2 \quad (3.1)$$

For the E (electric) and B (magnetic) fields at the LEP collider, this was equivalent to $P \approx 0.2\text{mW per electron}$. This may not seem like much, but even before

²The faster something goes, the slower time runs for it

³this is a technical term, as we'll discuss later

LEP was operating at its full potential the total synchrotron radiation output measured around thirteen megawatts⁴. Such losses can quickly become overwhelming, especially if we plan on detecting particles several orders of magnitude heavier than the Z boson.

Fortunately, the radiated power depends not just on the E and B fields, but on the mass of the particles being accelerated: from Equation 3.1 we can see that this dependence is $\sim 1/m^4$. If we accelerated protons instead of electrons, we decrease the radiated power by a factor of 10^{13} .

3.1 The Large Hadron Collider

The Large Hadron Collider (LHC)[lhcbrochure](#) is the premier proton collider in the world. It is the largest machine ever built, and has produced more particle data than all other experiments combined⁵. It is where we look for new particles.

The LHC is built in the same tunnel as the LEP, which it replaced, and turned on in 2007, initially colliding protons with a center of mass energy of 7 TeV. This energy was upgraded to 8 TeV in 2012, and it now operates with a center of mass energy of 13 TeV. A schematic of the LHC is shown in Figure 3.2. Protons are accelerated in stages, initially in a linear accelerator and then through a series of increasingly large circular synchrotrons until they can be injected into the LHC's main rings. The two proton beams are

⁴For reference, a modern locomotive produced about 6MW of power

⁵To the tune of 300 gigabytes of data a second, necessitating the largest computing grid in the world to handle. During its entire lifetime, LEP produced 400 TB of data. The LHC has already produced 130 PB.

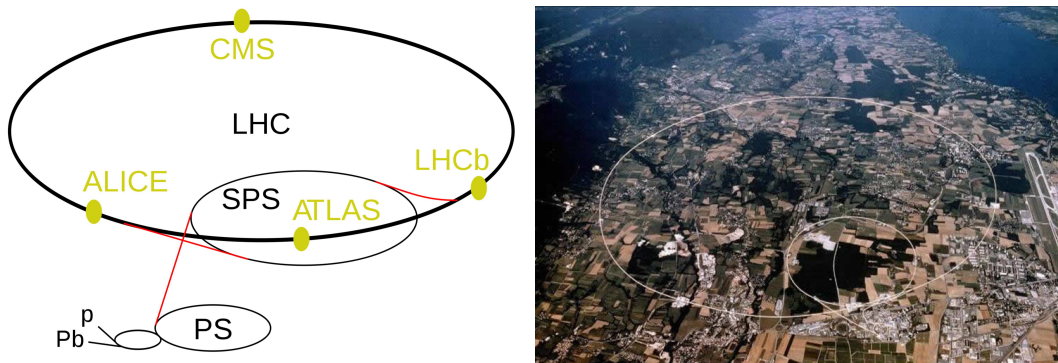


Figure 3.2: (left) Schematic of the LHC and the smaller accelerators which feed it. (right) True size of the LHC. The main ring has a circumference of 27 km. Lake Geneva can be seen in the top right of the picture.

identical other than the direction they travel in. The main rings are outfitted with 1,232 dipole magnets⁶ which keep the protons moving along the beam direction (and accelerate them) and 392 quadrupole magnets (which are used to focus the beam, see Figure 3.3). The enormous 7 Tesla magnetic fields necessary to handle these ultra-high-energy protons can only be achieved with superconducting magnets which must be cooled to below 2 Kelvin. The LHC requires almost 100 tonnes of superfluid liquid helium to remain operational. At its current collision energy, the protons reach a top speed of 99.9999999% the speed of light⁷. The beams are not continuous, but rather are composed of *bunches* of protons, each bunch containing roughly 115 billion protons.

The beams are made to cross at four experiments along the ring (see Figure 3.2). The spacing between bunches leaves 25 nanoseconds between crossings, equivalent to a collision rate of 40 MHz.

⁶a bar magnet is an example of a dipole magnet

⁷which is significantly faster than a Ferrari

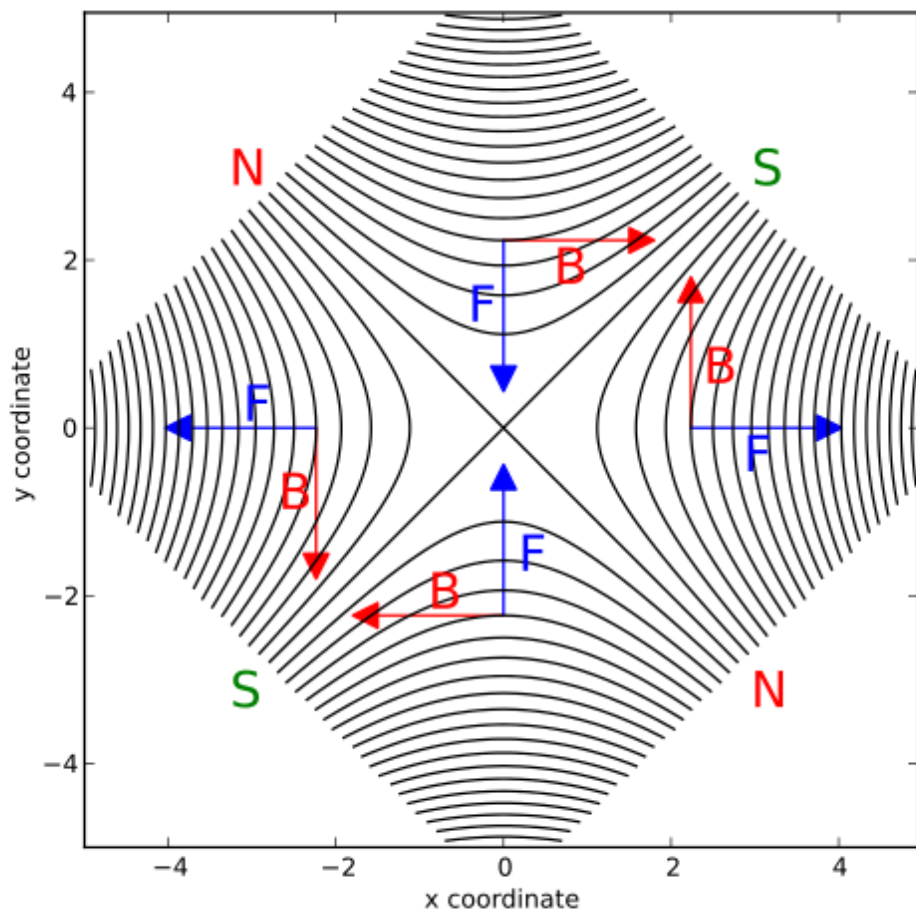


Figure 3.3: Quadrupole magnetic field, with the direction of the force felt by a charged particle in the field shown in blue. Alternating the N and S faces of the magnets allows the fields to focus a particle beam in both the vertical and horizontal directions.

3.1.1 A proton-proton Collision

Collision between electrons and positrons are easy to describe because both are point particles. Protons on the other hand, are composite. We usually talk about protons (and other hadrons like the neutron) as being composed of

three quarks. This however is not strictly true: when we say that the proton is made up of two up and one down quarks, we are naming the *valence* quarks of the proton. The proton is actually a complicated, ongoing interaction between those three quarks. The interaction is mediated by a web of gluons whose energy makes up the majority of the mass of the proton. And it's not one gluon per quark pair: the gluons interact with each other, spontaneously produce pairs of quarks from every generation, which decay back to gluons. As such, when we do smash two protons together with as much energy as the LHC provides, we aren't colliding protons, but rather, quarks or gluons (collectively called *partons*).

This can make measurements particularly difficult, as it's almost impossible to know what actually collided. Instead, we rely on the *Parton Distribution Function* (usually abbreviated as PDF⁸)[Bourilkov:2006cj; Ball:2014uwa](#) for a statistical understanding of what to expect. While we can never know, collision per collision, what actually interacted with what, we can simulate the collisions and create good models of what we expect to see.

Two example PDFs at different collision energies are shown in Figure 3.4. The 10 TeV collision PDF is representative of what we might see at the LHC⁹. The plots are read as follows: each curve represents a particle parton in a proton, and tells us the probability density¹⁰ of finding that parton carrying *momentum fraction* x . The momentum fraction is the fraction of the (longitudinal) momentum of the proton carried by that parton, so at the LHC

⁸which makes google searches for them very difficult

⁹currently operating at 13 TeV

¹⁰a quantum mechanical quantity easily converted to a probability

$x = 1$ would mean that parton with energy 6.5 TeV, $x = 0.1$ would be a parton with energy 0.65 TeV, and so forth¹¹. We are usually interested in events in

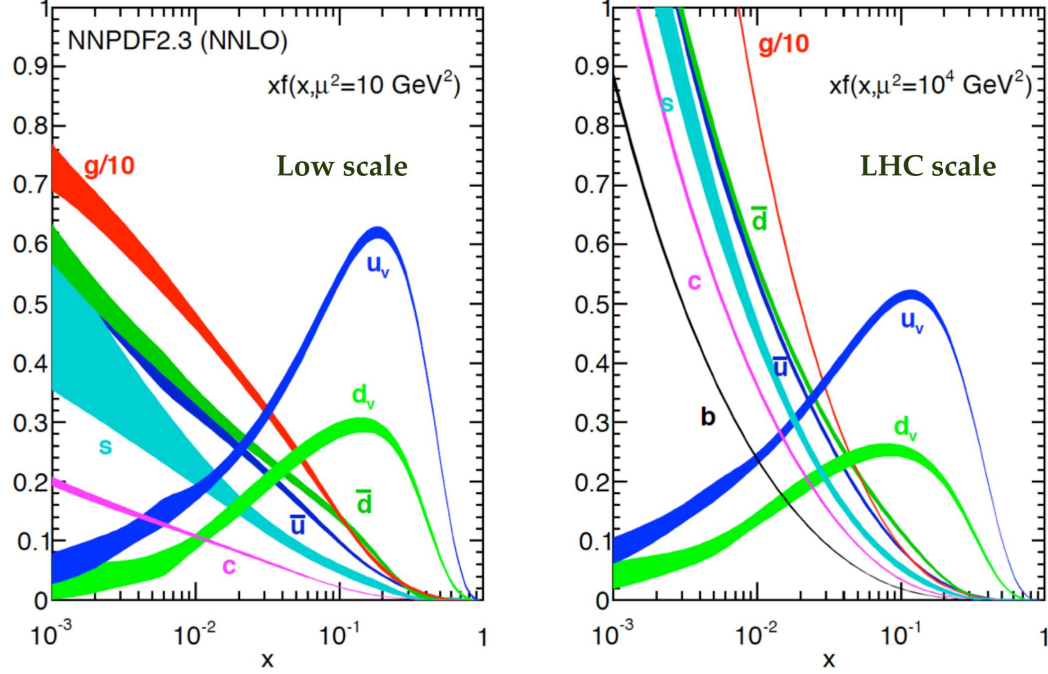


Figure 3.4: PDF for 10 GeV and 10 TeV collisions. Each curve represents a particle parton in a proton, and tells us the probability density of finding that parton carrying momentum fraction x .

which a large fraction of the total available energy is involved in the collision (At least, this is where we are most likely to find new physics). Each proton is governed by the PDFs, so in a collision between two protons we combine the probabilities. For example, from the Figure we see that at a low energy collider, if most of the energy of the protons is involved, there is a much higher chance of seeing a collision between two up quarks. This makes sense, as there are two up valence quarks in a proton. If we could somehow build a neutron-neutron collider, we would expect the down quark interactions

¹¹the beams at the LHC have combined energy of 13 TeV, so 6.5 TeV per beam.

to dominate. At higher energies, notice that the PDF for the gluon moves forward in x : at higher energies, we expect to see many more events with high energy that came from quark-gluon and gluon-gluon collisions.

Having correct PDFs is incredibly important for predicting the size of new physics signals at the LHC since many models have new particles which are only produced in specific interactions (our Z' for example is not created by gluon-quark interactions). Unfortunately, the PDFs are extraordinarily difficult to compute, so partial models are combined with large number of measurements at fixed target and collider experiments to hone in on their true values. Since these are inexact, we must assign systematic uncertainties to our simulations based on the variance between sets of “plausible” PDFs. This will be discussed in more detail in Section ??.

In two protons there are all the ingredients to create any particle in the standard model, as well as enough energy to access a lot of new physics. Even if the new physics is only accessible through the collisions of two bottom quarks, we can see from the PDFs that we expect bottom-bottom collisions carrying as high as 1.2 TeV of energy, easily high enough to probe new physics models. Such events would be a small signal compared to other collisions, but with a good detector, we should be able to sort them out from the backgrounds.

3.2 The Compact Muon Solenoid

The LHC collides protons at four experiments, each one-hundred meters below ground. Our analysis is performed on data collected by the Compact

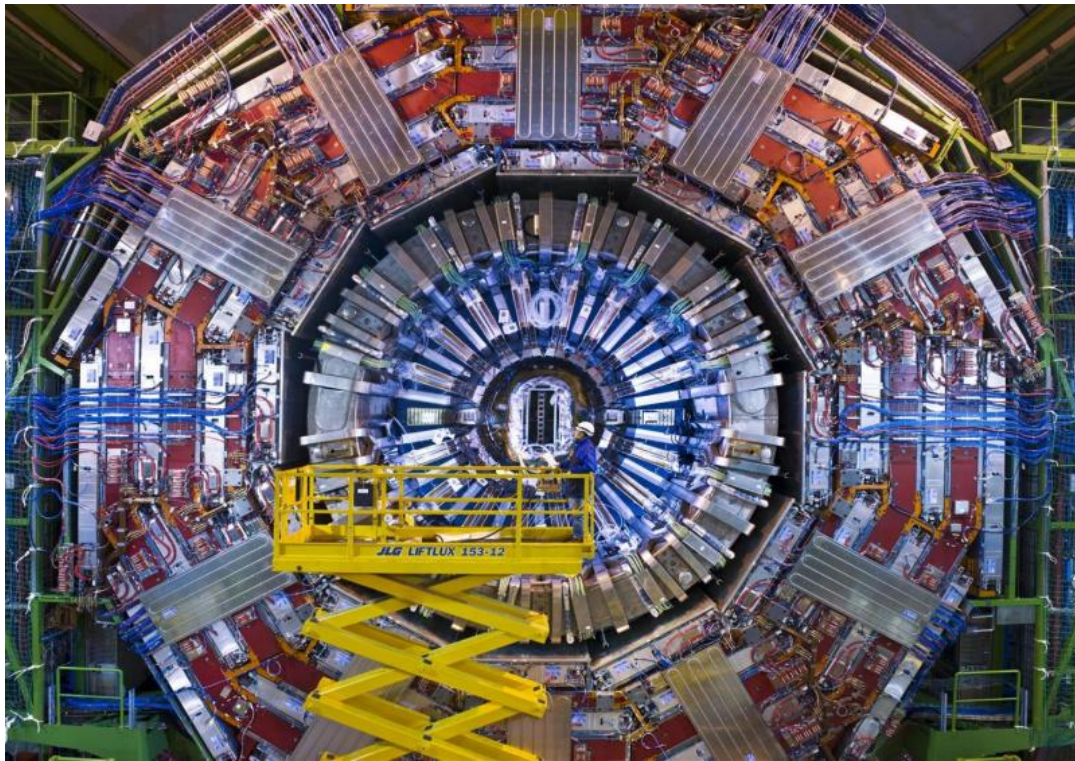


Figure 3.5: The Compact Muon Solenoid.

Muon Solenoid (CMS)[Bayatian:922757](#) Weighing in at 14,000 tons and run by a crew of almost 4,000 scientists, CMS may not seem compact, but it is the smaller (in volume) of the two main detectors on the LHC ring. A full description of its operation would easily fill an encyclopedia sized book, so we will just give a cursory overview: enough to understand how our analysis reconstructs collisions.

A slice of the detector is sketched in Figure 3.6.

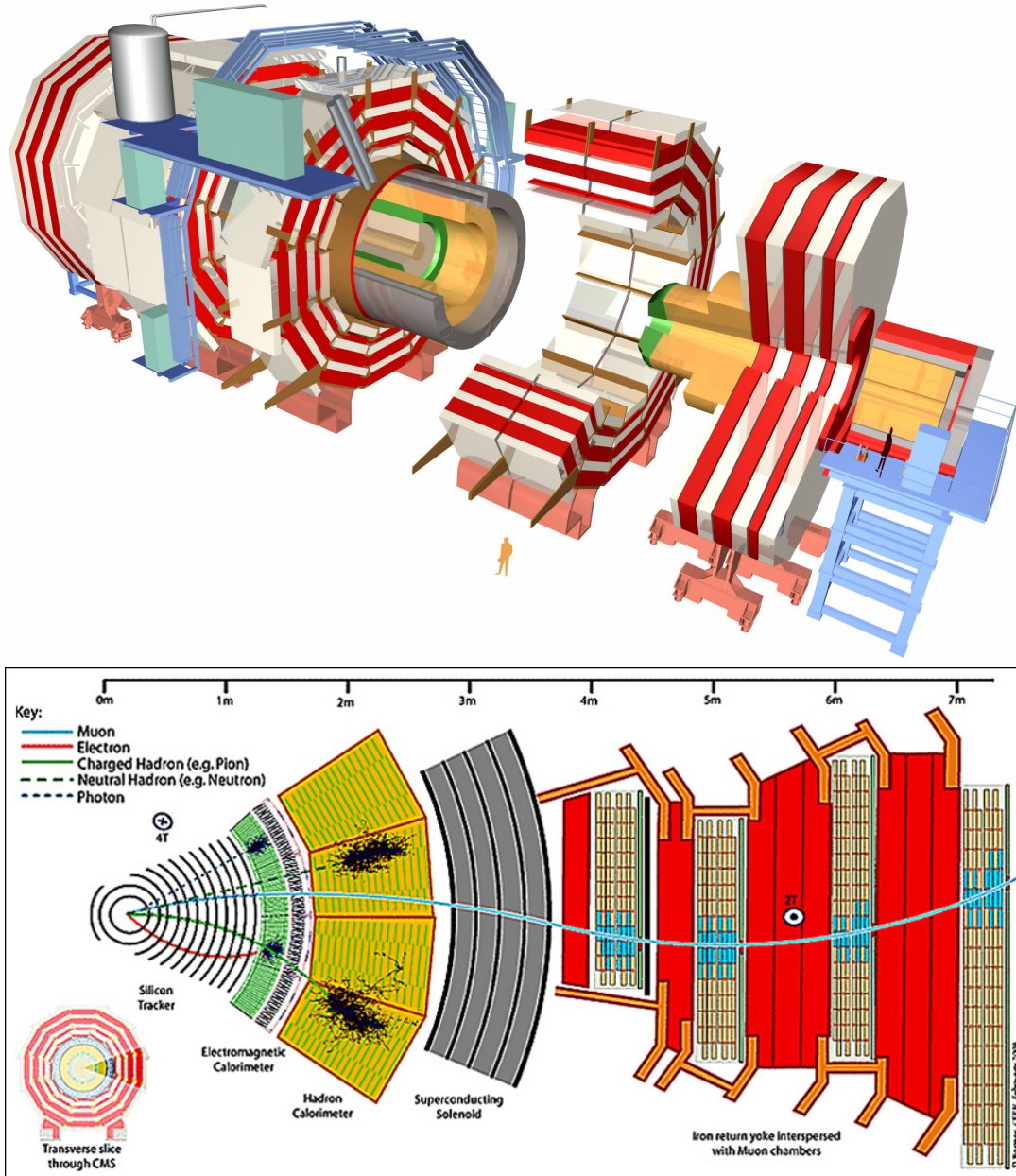


Figure 3.6: Schematic view of the CMS detector. Each portion is described in the text.

3.3 Coordinates

The CMS detector is essentially a large cylinder with concentric layers of detectors. The ends of the cylinder are also covered (we call these parts of the detector *the endcaps*). We define directions in the detector using two angles as in a modified spherical coordinate system: η and ϕ , where ϕ is the angle which sweeps our the circular component of the cylinder (and is therefore always perpendicular to the beam). η , the pseudorapidity is defined as:

$$\eta = -\ln \left(\tan \frac{\theta}{2} \right) \quad (3.2)$$

Where θ is the angle usually used alongside ϕ in spherical coordinates. $\eta = 0$ points straight out of the detector, while $\eta = \infty$ points directly along the beamline (see Figure 3.7). We use η instead of θ because differences in rapidity

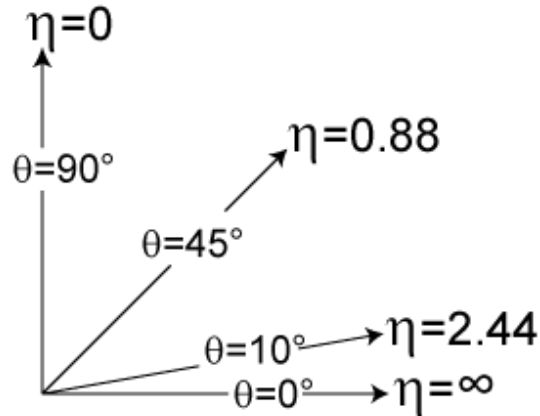


Figure 3.7: η and it's relation to θ .

are Lorenz Invariant¹², with the pseudorapidity being approximately so. This is very useful property, for while the protons in each beam have the same

¹²A Lorenz Invariant quantity is independent of the reference frame it is measured in.

energy, and are therefore symmetric in the laboratory rest frame, the partons which actually collide likely do not.

When we measure a particle in the CMS detector, we report three values: its radial angle, ϕ , pseudorapidity η and transverse momentum p_T . The transverse momentum is the momentum perpendicular to the walls of the cylinder. We rarely have cause to leave these coordinates, but we could recover Cartesian coordinates through the following transformations:

$$p_X = p_T \cos \phi, \quad p_Y = p_T \sin \phi, \quad p_Z = p_T \cosh \eta \quad (3.3)$$

The central axis (where the protons are in flight before the collision) is referred to as *the beam*.

3.3.1 The Subdetectors

3.3.1.1 The Tracker

The innermost layer of the detector is the Silicon Tracker. This sub-detector accurately measures the paths of charged particles as they zip through it. It is composed of 13 layers (14 in the endcaps). The first four layers are composed of silicon pixels, 66 million in total, each $100 \times 150 \mu\text{m}$ in area. The remaining layers are a cross-hatch of longer strips ($180 \mu\text{m}$ by 10 cm or 25 cm, depending on where they are). Taken all together this represents over 200 square meters of silicon sensors which enable us to measure the paths of particles by reconstructing series of “hits” in the pixels and strips. These *tracks* are determined with accuracies around $10 \mu\text{m}$.

Only charged particles interact with the silicon. The tracker is immersed

in a magnetic field (described below) which causes charged particles to curve. This curvature allows us to measure the charge and energy of particles. Unlike the calorimeters, the Silicon Tracker doesn't try to stop the charged particles, but rather, simply measures their momenta as they fly through it. It is our best tool for measuring the paths taken by the particles.

3.3.1.2 The Calorimeters

There are two Calorimeters: the Electromagnetic Calorimeter and the Hadron Calorimeter. Each operates on the same principle. They try to stop the majority of a particular kind of radiation, and measure the energy deposited. This allows us to measure the energy of the particles.

The Electromagnetic Calorimeter (ECAL) is composed of almost 80,000 lead-tungstate ($PbWO_4$) crystals. These crystals are a type of scintillator: a material which emit light when a particle deposits energy in it. Lead-Tungstate scintillates when a light charged particle (especially electrons) impact them. This light is proportional to the energy of the particle, and is collected to get a measure of the energy deposited. While photons have no charge, they can either pair produce electron-positron pairs, or directly interact with an electron in the crystal. For both electrons and photon processes, the initial radiation from the collision is typically energetic enough to interact several times in the crystal, producing a shower of electrons and light as byproducts of the initial interaction also cause scintillation. Heavier particles punch through these crystals leaving little energy. They are instead measured by the Hadronic Calorimeter.

The Hadronic Calorimeter (HCAL) (shown in Figure 3.8) consists of stacks of brass plates interlayered with plastic scintillator. The brass stops the hadrons, causing showers of secondary radiation which are detected by the scintillators. It is the only detector at CMS which can stop neutral particles (such as neutrons and many types of mesons), making it crucial for reconstructing events with hadronic activity.



Figure 3.8: The Hadronic Calorimeter, composed of 600 tons of brass, mostly recycled from WW2 naval shells.

3.3.1.3 The Solenoid

All three of these detectors are contained within a large solenoid¹³. This provides a field of 3.8 Tesla¹⁴. This field causes charged particle tracks to bend. The degree of this effect is dependent on the particle energy, which allows us to use the silicon tracker to measure the momentum of particles. The field is

¹³basically a really big electromagnet

¹⁴this is a powerful field! A bar magnet usually has strength measured in millitesla.

powerful enough to shift the alignment of the detector, an effect which must be properly accounted for. Brass is non-magnetic, explaining the choice to use it in the HCAL.

3.3.1.4 The Muon Chambers

The final detector layers are the Muon Chambers. Muons are too heavy to be stopped by the ECAL but not heavy enough to be stopped by the HCAL. Special detectors are instead used to detect them. There are three kinds of muon chambers, all of which operate on the same principle: as the muon traverses them, it knocks electrons off of gas atoms. These electrons are collected by the detector to measure the energy: the more electrons, the more energetic the muon.

3.3.2 The Particle Flow Algorithm

All the information from these subdetectors is collected and analyzed by the *Particle Flow Algorithm* (PFAlgorithm, or just PF)**CMS-PAS-PFT-09-001** This allows us to reconstruct events with a high level of certainty. The PF Algorithm leads to a gain especially in energy resolution for compound object, as can be seen in Figure 3.9. The PF is crucial for our ability to reconstruct *jets* which are described below.

Figure 3.9: Energy resolution gain from combining all information in the detector using the PF algorithm compared to that achievable with just the hadronic calorimeter.

3.3.3 Jets

In Chapter 1 we mentioned that colored particles cannot exist outside of a color-singlet state. When bare quarks are produced in proton-proton collisions they immediately begin the process of hadronization: creating new colored particles out of the vacuum until no color-states remain. Similarly, gluons created in proton-proton collisions must eventually decay to quarks, which in turn hadronize.

As a result of this, the LHC is unable to measure individual quarks, but instead, sees a shower of hadrons in the direction the original quark (or gluon) was moving. These showers, shown in Figure 3.10 are called *jets*. Jets are composed of constituents which are created by combining all the information available to the PF Algorithm mentioned above. Charged hadrons (such as π^+ , K^+ , etc) leave tracks in the silicon tracker and deposit energy in the hadronic calorimeter. Neutral hadrons (such as neutrons, π^0 , etc) do not leave tracks but deposit their energy in the hadronic calorimeter. Other particles may appear from decays of the hadrons: for example charged pions decay most commonly to $\mu\nu$ pairs and neutral pions usually decay to two high energy photons. These particles are measured by the muon chambers and electromagnetic calorimeter respectively and retained as constituents of the jet. Neutrinos don't interact with anything and their energy is therefore irrevocably lost.

Most events of interest at CMS produce more than one bare quark, and it is therefore not trivial to cluster the many possible constituents into the “correct” jets which faithfully reflect the underlying interaction. A number of algorithms

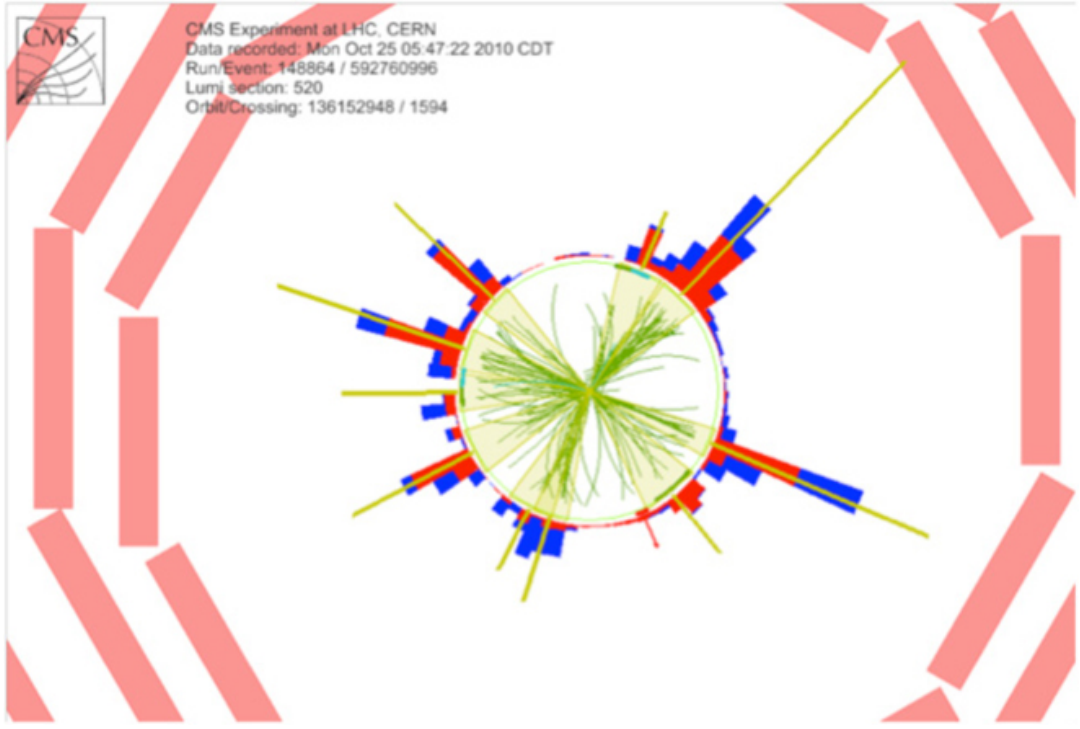


Figure 3.10: Typical CMS event with large number of hadrons (shown by the green lines). These hadrons are collected into *jets* (shown by yellow triangles). The PF algorithm combines information from the trackers and calorimeters to properly measure the total momentum of the jet.

exist. Four of the more common ones are shown in Figure 3.11. We exclusively use the *Anti- K_T* algorithm Cacciari:2008gp. The algorithm runs iteratively in the following fashion: Every *PF Candidate* (individual reconstructed particles) is considered against every other candidate and the distance-like parameter:

$$d_{ij} = \min(p_{T,j}^{-2}, p_{T,i}^{-2}) \frac{(y_i - y_j)^2 + (\phi_i - \phi_j)^2}{R^2} \quad (3.4)$$

is measured. Here R is a distance parameter which sets the size of the jet. The two closest constituents are paired together and become a new constituent. This pairing continues, adding new constituents to this and other *pseudo-jets* until $d_i B$ (where B is the beam) is equal to $1/p_T^2$ of a pseudo-jet. When this is

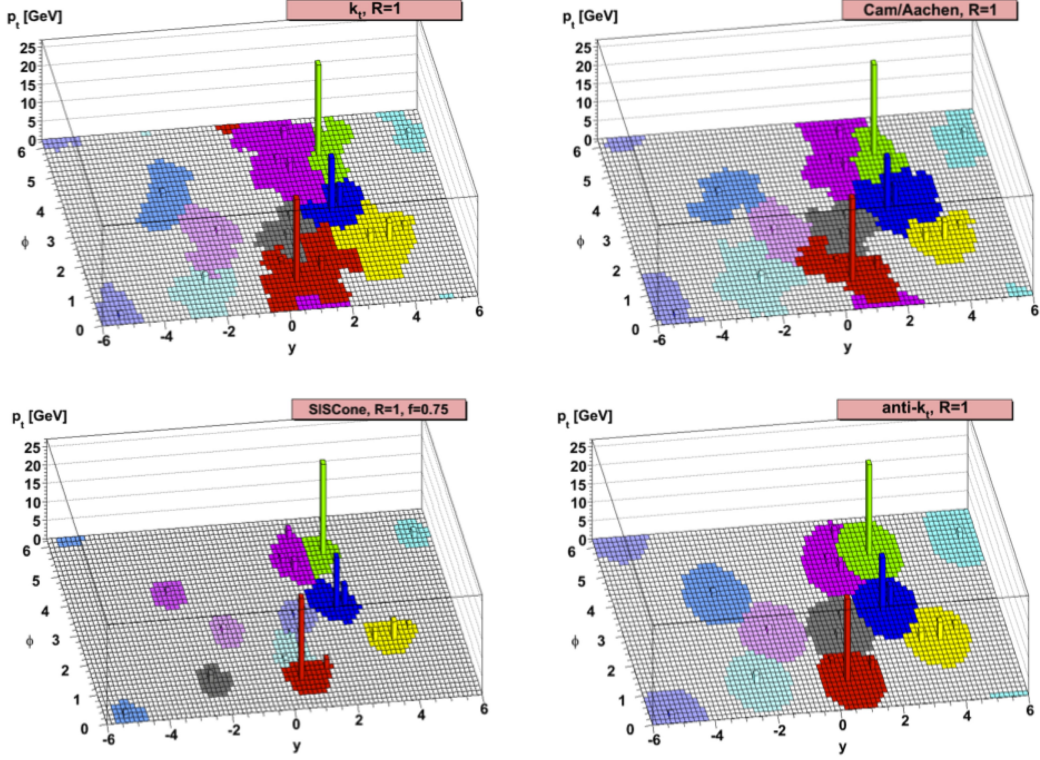


Figure 3.11: Four different *clustering* algorithms, each run on the same event. We use the *Anti- K_T* algorithm, described further in the text.

the case, that pseudo-jet is classified as a jet and it is removed from consideration. The algorithm continues for remaining constituents and pseudo-jets until no constituents remain.

The Anti- K_T algorithm is notable for creating “conical” jets with smooth, rounded edges (see again Figure 3.11) although this is not an exact statement, especially when two jets are near each other. We will refer to jets created with this algorithm as AKR jets, where R is the distance parameter used. We use two different kinds of jets in our analysis: AK8 and AK4, with R respectively 0.8 and 0.4. While it is impossible to reconstruct the small masses of most quarks, the energies and momentums of the jet can be used to measure their

kinematic properties. More massive particles such as the Higgs or W bosons and the very heavy top quark yield jets whose mass can be measured with some degree of accuracy. We use AK8 jets to reconstruct heavier objects.

3.3.4 Triggers

The detector output for each bunch-crossing would take approximately a megabyte to store. The crossing rate is forty megahertz, a rate well above what any modern computing system can handle. Because of this, the majority of collisions at CMS are discarded. The *trigger system* is responsible for pruning this output of uninteresting events.

The trigger operates in two main stages: the *Level 1* trigger is a hardware trigger. Detector output is stored in a buffer and analyzed by custom built FPGA circuits. This analysis looks for key markers of “interesting” physics such as a high energy muon, or very large deposits of energy in the HCAL or ECAL. This stage allows us to reject all but about 0.1% of collisions. The buffered data is released to the next stage, at a rate of around fifty kilohertz.

The *High Level* trigger takes the output of the Level 1 trigger and analyzes it further, separating interesting events for further study and rejecting all others. A large number of triggers are available, and there are further sorted into *Datasets* sharing a common characteristic. For example, the *Single-Muon* dataset consists of a large logical *or* of possible *High Level Trigger Paths*. Example of such paths include *HLT_Mu50* (an event with a 50 GeV muon), *HLT_Mu45Eta2p1* (an event with a 45 GeV muon in with $|\eta| < 2.1$) and others. Most triggers used in analysis attempt to keep all possible events, but *prescale*

Trigger are also kept, with only a fraction of triggering events allowed through. These triggers are used to measure the efficiency of the un-prescaled analysis triggers.

The resulting rate is about one kilohertz. There are the events which Physics Analyses are performed on. Our search for Z' will use two triggers: the *Mu45_eta2p1* trigger which collects events with one high energy (45 GeV) muon in the barrel of the detector, and the *El45_PFJet200_PFJet50* trigger, which collects events with one high energy electron (45 GeV) and at least two jets, one with energy at least 200 GeV and the other with energy at least 50 GeV.

Modeling the trigger is a crucial component of good simulations of the detector, especially when modeling new physics signals. Uncertainties in the overall efficiency of these triggers is an important systematics uncertainty of the analysis and will be further discussed.

3.3.5 Pileup

An *event* in CMS, ideally, is the outcome of a particular proton-proton collision. Most events do not yield any new physics or even “interesting” physics and the goal of our analysis will be to reduce the number of events in consideration to as small a set as possible.

Unfortunately, this ideal picture is not representative of the actual output of the detector because in each bunch-crossing there can be multiple proton-proton interactions. An event may therefore consist of up to forty individual interactions. It is therefore necessary to define a primary vertex: a *vertex* is

a point along the beam from which a large number of particle flow objects originate. The primary vertex is selected as the vertex with the highest value for the sum of the square of the transverse momenta of tracks and candidates associated with it.

Pileup can greatly affect the jet algorithms as particles produced in a vertex separate from the one we consider may be clustered into jets from the primary vertex. These *pileup contributions* smear out the measurements of jet mass and momentum and must be accounted for in the analysis. Specialized variables described in the next section can reduce these effects and better identify the mass of a jet. The choice of the AK4 and AK8 jet clustering algorithms is in part predicated on the resistance of that algorithm to effects from *soft* constituents (i.e. constituents from other vertices). This effect is shown in Figure 3.12

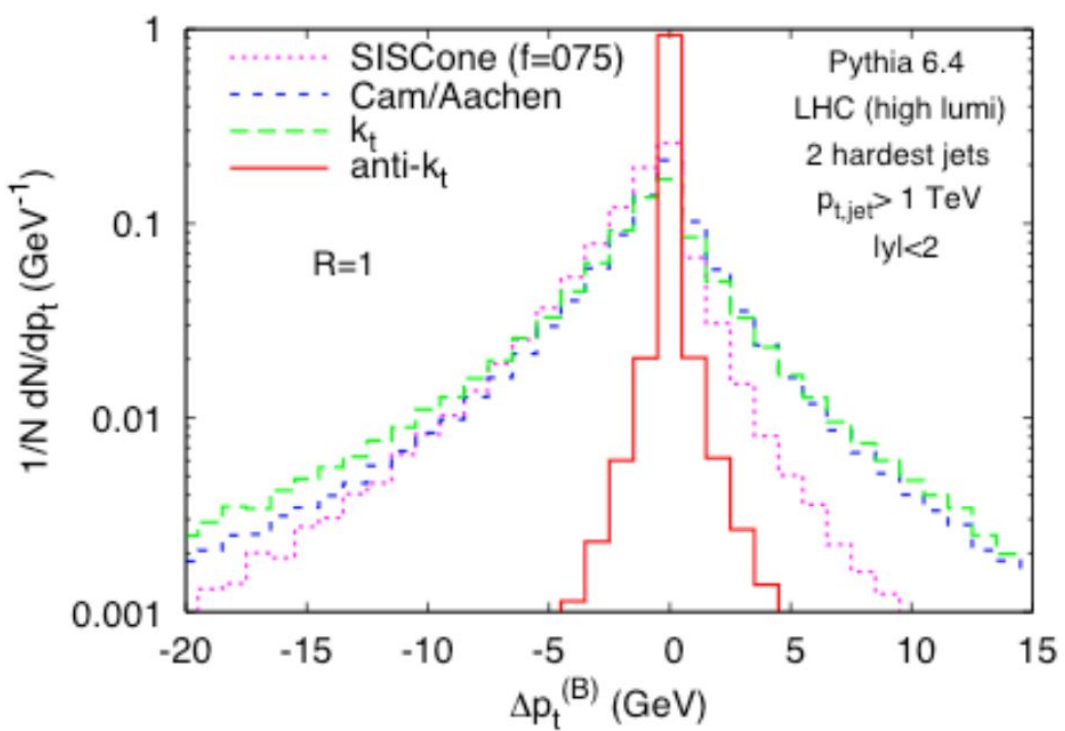


Figure 3.12: Resolution of $R = 1.0$ jets from different algorithms. The $Anti - K_T$ Algorithm performs best.

Bib

Alice Cocoros is great